Journal of Organometallic Chemistry, 417 (1991) 421–430
Elsevier Sequoia S.A., Lausanne
JOM 22007

Electrochemical reduction of $(\eta^3\text{-}C_3H_5)Fe(CO)_3X$ (X = Cl, Br, I) complexes. Evidence of formation of surface heterometallic compounds †

Domenico Osella *, Mauro Ravera

Dipartimento di Chimica Inorganica, Chimica Fisica e Chimica dei Materiali, Università di Torino, Via P. Giuria 7, 10125 Torino (Italy)

Sergei V. Kukharenko *, Vladimir V. Strelets

Academy of Sciences of the USSR, Institute of Chemical Physics, Laboratory of Metal Complex Electrocatalysis, Chernogolovka, Moscow Region, 142 432 (USSR)

Catherine E. Housecroft *

University Chemical Laboratory, Lensfield Road, Cambridge, CB2 1EW (UK)

(Received April 5th, 1991)

Abstract

The electrochemical reduction of the $(\eta^3\text{-}C_3H_5)Fe(CO)_3X$ (X = Cl, Br, I) complexes has been reinvestigated at both Pt and Hg electrodes by means of cyclic voltammetry. Quantum chemical calculations have been used to throw light on the nature of the frontier orbitals of $(\eta^3\text{-}C_3H_5)Fe(CO)_3Cl$ complex, and the results corroborate the proposed redox mechanism. The electrochemical behavior of the dimer $[(\eta^3\text{-}C_3H_5)Fe(CO)_3]_2$ has given some additional information on the actual redox mechanism. Some evidence of the formation of surface heterometallic products is reported.

Introduction

The electrochemical reduction of the allyltricarbonyliron complexes $(\eta^3\text{-}C_3H_5)Fe(CO)_3X$ (X = Cl, Br, I) has been studied by Gubin and Denisovich [1,2] by DC polarography at a dropping mercury electrode (DME). The polarograms of all the compounds exhibit two subsequent one-electron cathodic waves, the $E_{1/2}$ value of the second wave being almost independent of the nature of the halogen X. On the basis of the results and additional chemical studies [1], the first wave was judged to involve the reductive cleavage of the Fe–X bond, with subsequent formation of the

† Dedicated to the memory of Dr. Gabriela Teixeira, a dear colleague and friend.

0022-328X/91/$03.50

anion X^- and the radical $[(C_3H_5)Fe(CO)_3]^{\cdot}$, which is further reduced to the stable $[(C_3H_5)Fe(CO)_3]^-$ anion at the potential corresponding to the second wave.

The detailed mechanism of the electrochemical dehalogenation of organic halides RX is not only of theoretical but also of practical interest, and several metal complexes can catalyse such a process [3]. We therefore decided to undertake a study of the electrochemical behavior of the $(C_3H_5)Fe(CO)_3X$ (X = Cl, Br, I) series by means of cyclic voltammetry (CV) at either Pt or Hg electrodes in order to (i) understand better the chemical aspects of such redox processes and (ii) evaluate the role played by the mercury in stabilizing the electrode surface intermediates.

Quantum mechanical calculations by the Fenske–Hall method were also performed, and corroborate the proposed redox mechanism, as described below.

Results and discussion

The complexes $(C_3H_5)Fe(CO)_3X$ (X = Cl, Br, I) were made by a published procedure [4], involving the following reaction:

$$Fe_2(CO)_9 + CH_2{=}CH{-}CH_2X \rightarrow (C_3H_5)Fe(CO)_3X + Fe(CO)_5 + CO$$

The ^{1}H-NMR spectra of the complexes confirm the presence of *endo* and *exo* isomers, whose relative abundance depends on the nature of X [5]. However these isomers give indistinguishable CV responses. The structure of the compounds under study [6] is shown in Fig. 1.

Electrochemistry of $(\eta^3$-$C_3H_5)Fe(CO)_3X$ (X = Cl, Br, I) at a Hg electrode

Figure 2a shows the CV response of a THF solution of $(C_3H_5)Fe(CO)_3Br$ at a hanging mercury drop electrode (HMDE). In accord with the polarographic results [1], two cathodic peaks, A and B, of equal height, are observed, each exhibiting a directly associated reoxidation peak, C and D, respectively, in the reverse scan.

Analysis of the CV response [7] with the scan rate varied from 50 to 500 mV s^{-1} indicates that the first peak system A/D corresponds to an electrochemically quasi-reversible process (the $\Delta E_p = E_p(A) - E_p(D)$ values increases from 70 to 150 mV), and the second peak system, B/C, to a perfectly reversible process (the $\Delta E_p = E_p(B) - E_p(C)$ value is constantly equal to 60 mV). The i_p^a/i_p^c ratio of both the peak systems remains unity, suggesting full chemical reversibility for both processes. The other allyl complexes behave similarly. A change of solvent from THF to CH_2Cl_2 or CH_3CN does not significantly alter the behaviour. In the case of the coordinating CH_3CN solvent there is no evidence of any preceding chemical reaction (e.g. the departure of X^- to leave the cation $[(C_3H_5)Fe(CO)_3]^+$). Such behaviour has been observed for the isoelectronic $[(\eta^3$-allyl$)(\eta^5$-cyclopentadienyl$)CoX]$ complexes in acetonitrile [8].

The formal electrode potential values [7], $E^{\circ\prime} \approx (E_p^a + E_p^c)/2$, for the whole series are in keeping with the polarographic $E_{1/2}$ values [1] (Table 1). It can again be seen that the electrode potential of the second reduction step, assigned to the reduction of the radical $[(C_3H_5)Fe(CO)_3]^{\cdot}$ to the monoanion $[(C_3H_5)Fe(CO)_3]^-$, is almost independent of the nature of X. Furthermore, the potential does not change significantly if an excess of X^- is added to the solution (i.e. as Bu_4NX salts). In contrast the first peak system is profoundly affected by such an addition.

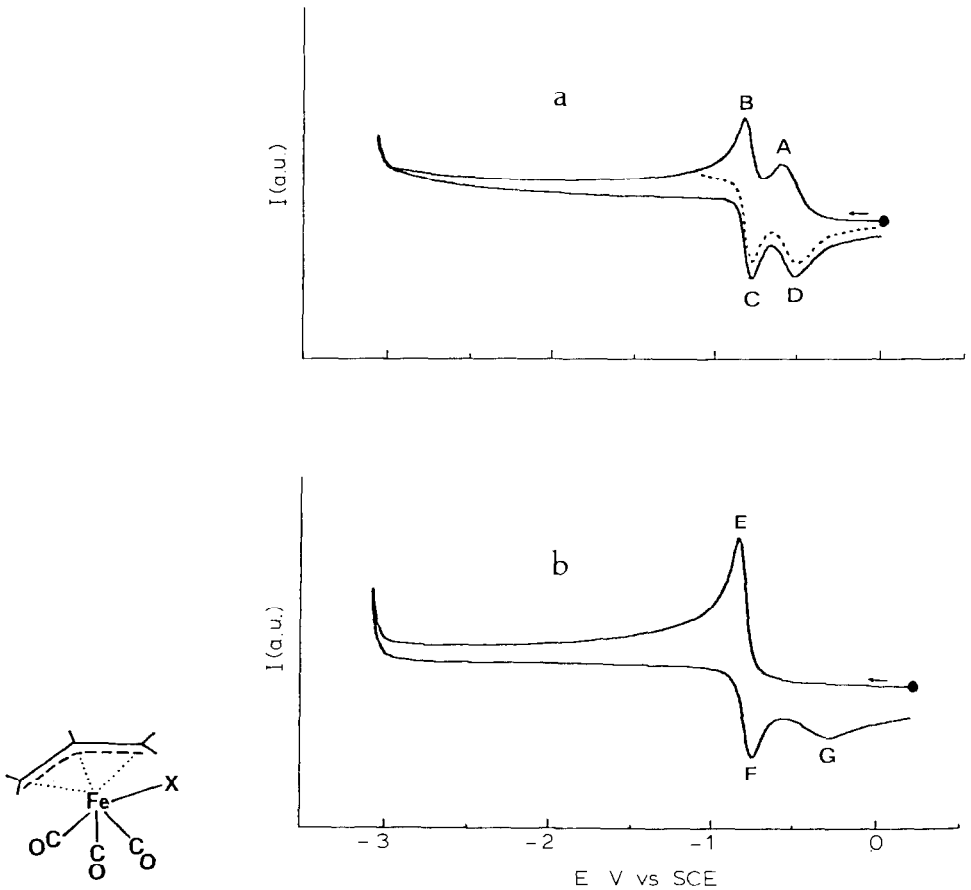

Fig. 1. Structure of $(\eta^3\text{-}C_3H_5)Fe(CO)_3X$ (X = Cl, Br, I).

Fig. 2. CV response of a THF solution of $(C_3H_5)Fe(CO)_3Br$ (0.2 m*M*) containing $[Bu_4N][PF_6]$ (0.05 *M*) at Hg electrode (a) and at Pt electrode (b). Room temperature, scan rate 200 mV s^{-1}; (○) starting potential.

Electrochemistry of $(\eta^3\text{-}C_3H_5)Fe(CO)_3X$ (X = Cl, Br, I) at a Pt electrode

Figure 2b shows the CV response of a THF solution of $(C_3H_5)Fe(CO)_3Br$ at a Pt electrode.

A cathodic peak E (at a potential near that of peak B, found in the previous experiment) is observed, followed in the reverse scan by a directly associated reoxidation peak F and by a broad peak G at a more positive potential. Analysis of the CV response with the scan rate varying from 50 to 500 mV s^{-1} exhibits the following features: (i) the difference between the potential of the cathodic and that of its directly associated reoxidation one, $\Delta E_p = E_p(E) - E_p(F)$, increases from 85 to 155 mV and (ii) the $i_p(F)/i_p(E)$ ratio remains close to 0.5, throughout.

Exhaustive electrolysis carried out at a working potential beyond peak E (E_w = −1.0 V) at a Pt basket macroelectrode consumes 2 Faradays/mole of

Table 1

Redox electrode potentials of the $(\eta^3\text{-}C_3H_5)Fe(CO)_3X$ (X = Cl, **1**; Br, **2**; I, **3**) series and for the dimer $[(C_3H_5)Fe(CO)_3]_2$ (**4**) in various solvents containing $[Bu_4N][PF_6]$ (0.05 *M*) at 20 °C

compound	peaks/s	electrode material	$E^{\circ\prime}$ (V vs. SCE)		
			CH_3CN	CH_2Cl_2	THF
1	A/D	Hg	−0.42	−0.31	−0.60
	B/C	Hg	−0.69	−0.66	−0.78
	E/F	Pt	−0.73	−0.80	−0.77
	G	Pt	−0.10	+0.12	−0.25
2	A/D	Hg	−0.39	−0.26	−0.54
	B/C	Hg	−0.69	−0.66	−0.78
	E/F	Pt	−0.66	−0.64	−0.79
	G	Pt	−0.15	−0.01	−0.24
3	A/D	Hg	−0.37	−0.22	−0.57
	B/C	Hg	−0.69	−0.66	−0.78
	E/F	Pt	−0.65	−0.64	−0.77
	G	Pt	−0.16	−0.09	−0.22
4	H/L	Hg	–	–	−0.78
	I	Hg	–	–	−2.14
	H/L	Pt	–	–	−0.78
	I	Pt	–	–	−2.40

[a] For the reversible processes, the $E^{\circ\prime}$ value ($E^{\circ\prime} \approx (E_p^c + E_p^a)/2$) is reported along with the indication of the peak system. For irreversible processes, the E_p value is reported at a scan rate of 200 mV s^{-1} along with the indication of the peak. See the text and the Figures for the peak labeling scheme.

$(C_3H_5)Fe(CO)_3Br$. Furthermore, EPR monitoring clearly indicates that the $[(C_3H_5)Fe(CO)_3]^{\cdot}$ radical is formed at the beginning of the reduction [9*].

Similar behaviour was found for the other complexes of the series in THF, CH_2Cl_2 or CH_3CN solvents (Table 1).

On the basis of these results we propose the following redox scheme at a Pt electrode:

$$(\eta^3\text{-}C_3H_5)Fe(CO)_3X \underset{E_1}{\overset{e}{\rightleftharpoons}} (\eta^3\text{-}C_3H_5)Fe(CO)_3X^{\cdot} \xrightarrow{-X^-} (\eta^3\text{-}C_3H_5)Fe(CO)_3^{\cdot}$$

$$(\eta^3\text{-}C_3H_5)Fe(CO)_3^{\cdot} \underset{E_2}{\overset{e}{\rightleftharpoons}} (\eta^3\text{-}C_3H_5)Fe(CO)_3^-$$

where $E_2 \approx E_1$, so that the two steps fully overlap in the CV response. The nature of the electrode reaction corresponding to the irreversible anodic peak G, observed in the reverse scan, will be discussed later.

The large difference in the redox behavior of the $(C_3H_5)Fe(CO)_3X$ complexes at the Hg and Pt electrode provides unambiguous evidence for the involvement of the Hg in the first reduction step [11]. The interaction of $(C_3H_5)Fe(CO)_3X$ with the Hg surface facilitates the first reduction process. In the absence of such an interaction,

* Reference number with asterisk indicates a note in the list of references.

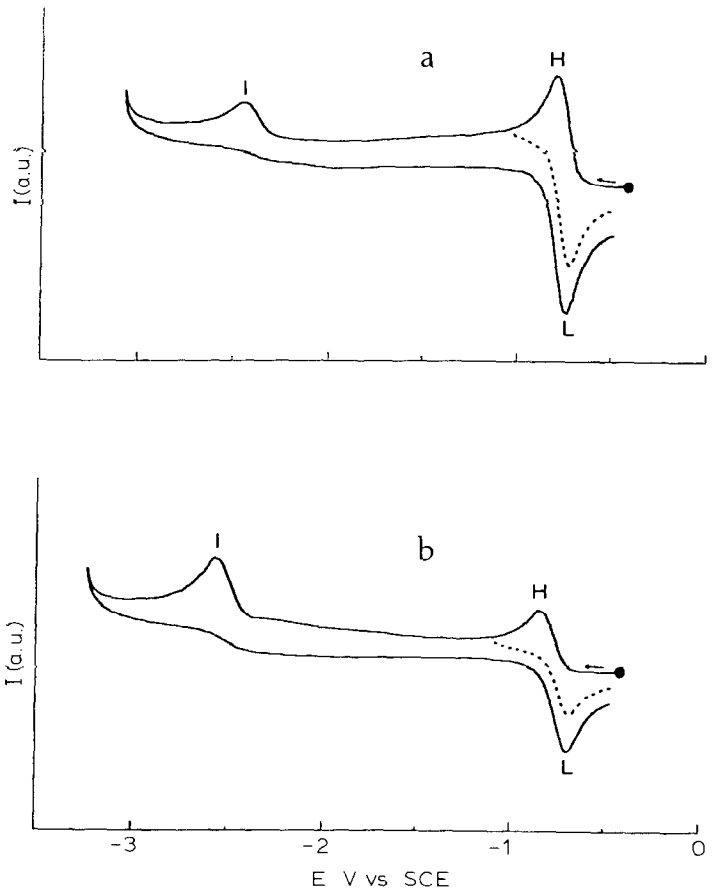

Fig. 3. CV response of a THF solution of $[(C_3H_5)Fe(CO)_3]_2$ (0.5 m*M*) containing $[Bu_4N][PF_6]$ (0.05 *M*) at Pt electrode, at room temperature (a) and at $-35\,^{\circ}C$ (b). Scan rate 200 mV s^{-1}; (○) starting potential.

i.e. at Pt electrode, the first reduction is shifted to a more negative potential (200–250 mV) and the corresponding peak overlaps with the second.

In order to clarify this point we examined the electrochemical behavior of $[(C_3H_5)Fe(CO)_3]_2$. This dimer was obtained by means of zinc dehalogenation [12] of the iodine complex:

$$2(C_3H_5)Fe(CO)_3I + Zn \rightarrow [(C_3H_5)Fe(CO)_3]_2 + ZnI_2$$

Electrochemistry of $[(\eta^3\text{-}C_3H_5)Fe(CO)_3]_2$ at a Pt and at a Hg electrode

Figure 3 shows the CV response of a THF solution of $[(C_3H_5)Fe(CO)_3]_2$ at a Pt electrode at $20\,^{\circ}C$ (Fig. 3a) and at $-35\,^{\circ}C$ (Fig. 3b), respectively.

At room temperature a cathodic peak H is observed, exhibiting a directly associated reoxidation peak L ($\Delta E_p = 70$ mV, $i_p^a/i_p^c = 1$ at 200 mV s^{-1}, *dashed line* in Figure 3). At a more negative potential a small, irreversible cathodic peak I is also observed. When peak I is traversed, the current intensity of peak L increases, i_p^a/i_p^c being > 1 (*solid line* in Figure 3). As the temperature is lowered from 20 to $-35\,^{\circ}C$ the first reduction peak, H, decreases and the second one, I, increases; this

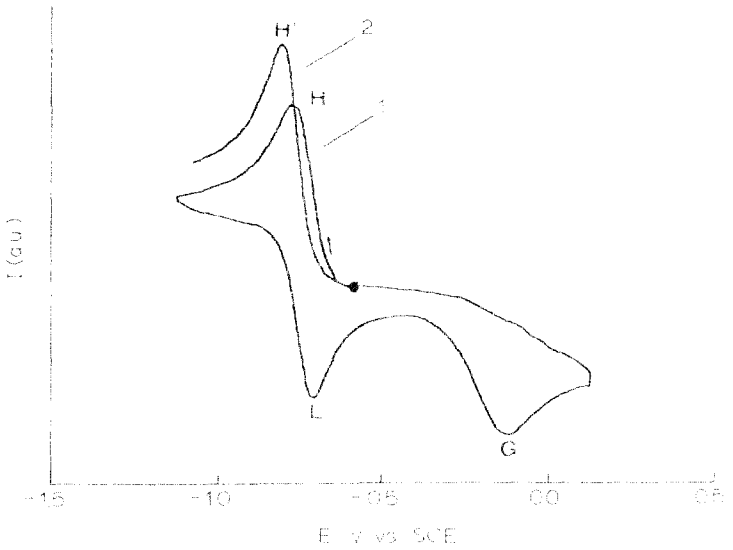

Fig. 4. CV response of a THF solution of $[(C_3H_5)Fe(CO)_3]_2$ (0.5 m*M*) containing $[Bu_4N][PF_6]$ (0.05 *M*) in the presence of 1.0 m*M* $[Bu_4N]Br$ at Pt electrode and at room temperature. 1- first scan, 2-second scan. Scan rate 200 mV s^{-1}; (→) starting potential.

behavior is accompanied by a change in colour from green to bright red, and arises from the well established [10,12] equilibrium between the radical monomer $[(C_3H_5)Fe(CO)_3]^{\cdot}$ (green) and the dimer $[(C_3H_5)Fe(CO)_3]_2$ (red). Indeed, at $-35\,^{\circ}C$ the intensity of the EPR signal of the radical monomer is much lower. These features unambiguously indicate that the peak system H/L corresponds to the one-electron reduction of the radical $[(C_3H_5)Fe(CO)_3]^{\cdot}$ and peak I corresponds to the two-electron reduction of the dimer $[(C_3H_5)Fe(CO)_3]_2$. The relative abundance of the two species in solution depends on the temperature. The electrochemical behaviour at a Hg electrode is similar, but the potential corresponding to peak I is ca. 260 mV more positive for the Hg electrode than for the Pt electrode. This may be due to the absorption of the dimer on Hg with the formation of $[(C_3H_5)Fe(CO)_3]_2Hg$. Formation of an analogous compound, namely $[(C_3H_5)Fe(CO)_2]_2Hg$, was observed in the reduction of $(\eta^5\text{-}C_5H_5)Fe(CO)_2X$ (X = Cl, Br, I) at a Hg electrode [13].

Electrochemistry of $[(\eta^3\text{-}C_3H_5)Fe(CO)_3]_2$ in the presence of Br^-

Figure 4 shows the CV response of a THF solution of $[(C_3H_5)Fe(CO)_3]_2$ at a Pt electrode in the presence of an excess of $[Bu_4N]Br$ at room temperature.

The reversible one-electron peak system H/L is still observed, corresponding to the reduction of the radical. On the reverse scan, at more positive potentials, an irreversible oxidation peak G (exactly coincident with that of the $(C_3H_5)Fe(CO)_3Br$ complex previously discussed) is also found. Furthermore, in the second reduction scan the cathodic peak (now labelled as H′) increases in height [14*] and moves to a slightly more negative potential and is then exactly coincident with peak E in the CV response of $(C_3H_5)Fe(CO)_3Br$ complex. All these features indicate that the anodic peak G corresponds to the oxidation of the radical $[(C_3H_5)Fe(CO)_3]^{\cdot}$ in the

presence of Br^- (in the bulk solution in the present experiment or absorbed on the electrode surface in the previous one) to form $(C_3H_5)Fe(CO)_3Br$, which in turn undergoes a two electron reduction to $[(C_3H_5)Fe(CO)_3]^-$ and Br^- (at the potential of peak H′ in the second cathodic sweep).

Interestingly, the CV response of $[(C_3H_5)Fe(CO)_3]_2$ at a Hg electrode in the presence of Br^- is similar to that of $(C_3H_5)Fe(CO)_3Br$ at the same electrode.

Attempts to identify the Hg intermediate

The interaction of $(C_3H_5)Fe(CO)_3X$ (X = Cl, Br, I) with a Hg electrode should result in the oxidative addition of the FeX bond at Hg, which will facilitate the first reduction step. A precedent can be found in the electrochemical behavior of RHgX complexes at a Hg electrode, which results in the formation of an "organic calomel" RHgHgX compound [15].

In an attempt to produce a similar intermediate in solution the anion $[(C_3H_5)Fe(CO)_3]^-$ was treated with $HgCl_2$ in THF. The immediately-formed light brown product decomposed within a few minutes to the yellow $(C_3H_5)Fe(CO)_3Cl$ complex with precipitation of Hg, as indicated below:

$$[(C_3H_5)Fe(CO)_3]^- + HgCl_2 \rightarrow \text{“}(C_3H_5)Fe(CO)_3HgCl\text{”} + Cl^- \downarrow (C_3H_5)Fe(CO)_3Cl + Hg$$

We therefore propose the formation at the electrode surface of a similar product formed by partial insertion of Hg into the Fe–X bond, as shown in Fig. 5.

When the reaction proceeds and the Fe–X bond is broken, the anion X^- remains on the electrode surface long enough to permit the reoxidation of $[(C_3H_5)Fe(CO)_3]^{\cdot}$ to $(C_3H_5)Fe(CO)_3X$. The same situation holds for the Pt electrode, with a minor degree of Fe–X bond activation and chemical reversibility.

Theoretical calculations

The bonding in $(C_3H_5)Fe(CO)_3X$ (X = halogen) was investigated for the case of X = Cl as a representative compound. The bonding was considered in terms of the interaction of the allyl fragment $[C_3H_5]^-$ with $[Fe(CO)_3Cl]^+$. The interfragment interaction is a simple one, and is summarised in the correlation diagram shown in Fig. 6. As expected there are two major orbital interactions: 67% of the total Mulliken overlap population arises from an interaction of the non-bonding MO of $[C_3H_5]^-$ with the LUMO of the $[Fe(CO)_3Cl]^+$ fragment and 31% from the interaction of the allylic π-bonding orbital with the low lying σ-orbital of the metal.

In the context of the electrochemical results reported here it is the characteristics of the low lying MO's of $(C_3H_5)Fe(CO)_3X$ that are of interest. For X = Cl, the LUMO exhibits Fe–Cl σ^* character [16]. However, the calculations also show that a second unoccupied MO lies 0.8 eV above the LUMO and that this orbital possesses

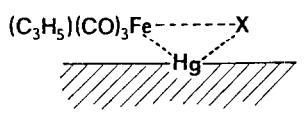

Fig. 5. Sketch of the surface heterometallic compound suggested to be formed during the reduction of $(C_3H_5)Fe(CO)_3X$ at a Hg electrode.

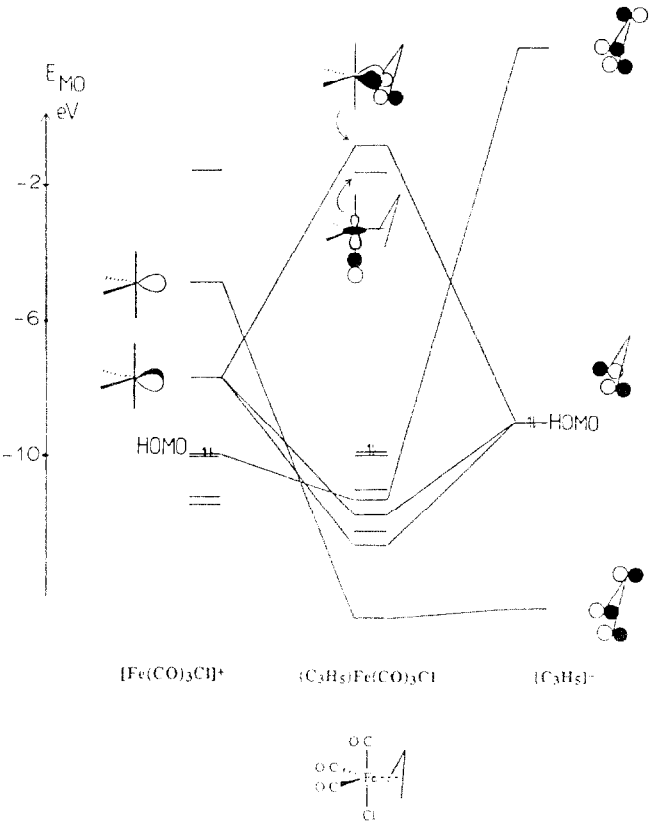

Fig. 6. MO correlation diagram for the interaction of the fragments $[Fe(CO)_3Cl]^+$ and $[C_3H_5]^-$. The characteristics of the lowest unoccupied MO's of $(C_3H_5)Fe(CO)_3Cl$ are also depicted.

Fe–allyl antibonding character. Although the results are consistent with the fact that occupation of the LUMO upon electrochemical reduction would lead to a weakening of the Fe–Cl bond, they do not rule out the possibility that reduction might cause a perturbation of the metal–allyl bonding. Thus, the experimentally observed reductive cleavage of the Fe–X bond is favoured by the interaction with the electrode material.

Final remarks

(i) On the Pt electrode the $(C_3H_5)Fe(CO)_3X$ (X = Cl, Br, I) species are reduced in a two-electron step (E_1CE_2 mechanism where $E_1 \approx E_2$) with Fe–X bond cleavage (C step) and formation of the $[(C_3H_5)Fe(CO)_3]^{\cdot}$ radical, which is further reducible to the closed-shell $[(C_3H_5)Fe(CO)_3]^-$ anion.

(ii) The chemical interaction of $(C_3H_5)Fe(CO)_3X$ (X = Cl, Br, I) compounds with Hg electrode results in the formation of unstable heterometallic $\{(C_3H_5)Fe(CO)_3HgX\}$ complexes, which are reduced at a potential 200 ÷ 250 mV more positive than the original complexes.

Experimental section

The complexes $(C_3H_5)Fe(CO)_3X$ (X = Cl, Br, I) were made by a published procedure [4]. The purity of each was checked by IR and ^1H-NMR spectroscopy.

The EPR spectra were recorded on a Varian E-109 instrument operating in the X-band mode and equipped with a variable-temperature accessory. Varian pitch ($g = 2.0028$) was used as reference standard for g values calibration.

The voltammetric measurements were performed on two types of apparatus: (i) a PAR model 173 potentiostat driven by a PAR model 175 universal programmer (Moscow) and (ii) a PAR model 273 electrochemical analyzer connected to an interfaced IBM microcomputer (Turin). All the potentials are relative to a saturated aqueous Calomel Electrode (SCE) and calibrated against the ferrocene (0/1 +) couple [17].

The construction of the electrochemical cell for low temperature voltammetric measurements and the purification of solvents and supporting electrolytes were as previously described [18].

Fenske–Hall molecular orbital calculations [19] were carried out on $(C_3H_5)Fe(CO)_3Cl$ using crystallographically determined coordinates [6] for the bromo-analogue. The Fe–Cl distance was set at 2.40 Å. The calculations employed single-ζ Slater function for the 1s and 2s function of C and O. The exponents were obtained by curve fitting double-ζ function of Clementi [20]; double-ζ function for the $2p$ orbitals were used directly. An exponent of 1.16 was used for H.

Acknowledgments

We thank the Council of National Research (CNR, Rome) and the MURST (Rome) for financial support, Professor E. Giamello (University of Turin) for recording the EPR spectra, and Professor S. Roffia (University of Bologna) for useful discussions. M.R. thanks the European Economic Community (EEC) for the grant of a studentship under the ERASMUS scheme.

References

1 S.P. Gubin and L.I. Denisovich, J. Organomet. Chem., 23 (1968) 477.
2 S.P. Gubin, Pure Appl. Chem., 23 (1970) 463.
3 O.N. Efimov and V.V. Strelets, Coord. Chem. Rev., 99 (1990) 15.
4 H.D. Murdoch and E. Weiss, Helv. Chim. Acta, 45 (1962) 1927.
5 J.W. Faller and M.A. Adams, J. Organomet. Chem., 170 (1979) 71.
6 F.E. Simon and J.W. Lauher, Inorg. Chem., 19 (1980) 2338.
7 (a) A.J. Bard and L.L. Faulkner, in Electrochemical Methods, Wiley, New York, 1980; (b) E.R. Brown and J.R. Sandifer, in B.W. Rossiter and G.F. Hamilton (Eds.), Physical Methods of Chemistry, Wiley, New York, 1986.
8 S. Roffia, C. Paradisi, G. Teixeira and T. Aviles, Preceedings of Congress Interdivisionale della Societé Chimice Italiena 89, Perugia (Italy), 7–11 October 1989, p. 596.
9 The room temperature X-band EPR spectrum of a partially electrolyzed (0.5 Faraday/mole, $E_w = -0.7$ V) CH_2Cl_2 solution of $(C_3H_5)Fe(CO)_3Br$ containing $[Bu_4N][PF_6]$ (0.2 M) exhibits a broad absorption at $g = 2.0458$ without any hyperfine coupling. This g value is very similar to that reported for the $[(C_3H_5)Fe(CO)_3]^{\cdot}$ radical in benzene [10].
10 H.D. Murdoch and E.A.C. Lucken, Helv. Chim. Acta, 47 (1964) 1517.
11 S.W. Blanch, A.M. Bond and R. Colton, Inorg. Chem., 20 (1981) 755.

12 C.F. Putnik, J.J. Welter, G.D. Stucky, M.J. D'Aniello Jr., B.A. Sosinsky, J.F. Kirner and E.L. Muetterties, J. Am. Chem. Soc., 100 (1978) 4107.
13 D. Mihalovà and A.A. Vlcek, Inorg. Chim. Acta, 43 (1980) 43.
14 The height of peak H′ is less than that expected for a two-electron reduction process. This may be due to the diffusion of $(C_3H_5)Fe(CO)_3Br$ complex (formed in the first scan) away from the electrode.
15 V.V. Pinyackin, A.L. Chistyakov and I.V. Stankevic, Metalloorg. Khim., 4 (1991) 180.
16 R.B. King, Trans. N. Y. Acad. Sci., 28 (1966) 889.
17 G. Gritzner and J. Kuta, Pure Appl. Chem., 54 (1982) 1527.
18 S.V. Kukharenko, Ph.D. Thesis, Institute of Chemical Physics, Chernogolovka, 1989.
19 (a) M.B. Hall and R.F. Fenske, Inorg. Chem., 11 (1972) 768;
(b) M.M. Kostic and R.F. Fenske, Organometallics, 1 (1982) 974.
20 E. Clementi, J. Chem. Phys., 40 (1964) 1944.